JSML
Journal of Science and Mathematics Letters
ISSN 2462-2052 • eISSN 2600-8718

Research Article

Design, Simulation, and Fabrication of a Fractal Square Microstrip Antenna Based on Spiral Slots with Dual-band Feature

Akeel Sami Tahir[1], Doha Al-Feadh[1], Wa'il A. Godaymi Al-Tumah[1]*, Alistair P. Duffy[2]

[1] Department of Physics, College of Science, University of Basrah, 61004, Basrah, Iraq
[2] Department of Electrical Engineering, Computing, Engineering and Media, De Montfort University, LE1 9BH UK, Leicestershire, United Kingdom
* Corresponding author: wail.godaymi@uobasrah.edu.iq

ARTICLE HISTORY

Received
3 November 2025
Revised
2 February 2026
Accepted
15 February 2026
Published
22 February 2026

KEYWORDS

Microstrip Antennas
Square Patch
Fractal Antennas
HFSS Software
C-bands
Dual band

ABSTRACT

Microstrip antennas offer versatile operational capabilities, including wideband, dual-band, multiband, and compact configurations, depending on the geometry of the radiating patch. Fractal concepts have emerged as an effective approach for reconfiguring antenna patches to enhance bandwidth and multiband performance. In this study, a novel fractal-patch microstrip antenna is proposed to achieve wideband characteristics suitable for multifunctional wireless communication applications. The antenna employs a square fractal patch incorporating etched spiral slots and semicircular cuts at each corner, with overall dimensions of 79 × 50 × 1.59 mm³. The design was simulated using Ansoft High Frequency Structure Simulator (HFSS) based on the finite element method (FEM). Key performance parameters, including input impedance, return loss, voltage standing wave ratio (VSWR), gain, surface current distribution, and radiation patterns, were analysed. The proposed antenna demonstrates dual-band characteristics, resonating at 4.23 GHz and 7.13 GHz within the C-band region. Simulated results show VSWR values of 1.17 and 1.06 at 4.01 GHz and 7.10 GHz, respectively, indicating good impedance matching and stable radiation performance. Fabricated antenna measurements were conducted and compared with simulation results, showing satisfactory agreement. The proposed fractal-patch microstrip antenna exhibits reliable dual-band operation and favourable radiation characteristics, making it suitable for C-band applications such as satellite communication, internet telecommunication, and mobile feeder systems. Its stable performance under varying weather conditions further supports its potential for practical wireless communication services.

https://doi.org/10.37134/jsml.vol14.1.14.2026

1. INTRODUCTION

In the modern world, the development of communication systems, including antennas, has led to a wide shift in the areas of their use. This development highlighted the importance of seeking ease of manufacture and low cost in the small size of the antennas. Microstrip antennas (MSAs) are considered among one of the available choices because they had these advantages, in addition to their use in radar and wireless communication systems (James & Hall, 1989). MSA concept was first proposed in 1953 (Deschamps, 1953). later the practical antenna was developed in the 1970, where the basic structure of MSA comprises a ground plane on the bottom side of the dielectric substrate and a radiating patch on the top side (Howell, 2003). The wide use of MSAs requires a continuous improvement in their characteristics to including most applications, especially in terms of gain and bandwidth, being the main weaknesses of MSA (Karanam & Kakkar, 2025; Sharma et al., 2019). However, the majority of wireless communication systems' bandwidth requirements cannot be met by MSA alone. The addition of one or more resonant structures to MSA design is the most general idea behind bandwidth improvement approaches (Muthuvalu & Sulaiman, 2010). These extra segments could take the shape of different patches or slots.

The limited bandwidth and poor gain of MSA restrict its practical use. A thick or foam substrate (David, 1995), the creation of slots or notches like in U-shaped, E-shaped, or H-shaped patch antennas (Wa'il et al., 2020; Gao et al., 2013; Nguyen et al., 2012), and the utilization of two layer electromagnetically connected stacked structures (Srivastava et al., 2009) are just a few methods that have been employed to expand the patch antenna's bandwidth. Many wide-band and dual-frequency antennas employing layered structures have been described. Dual band is displayed via a rectangle patch filled with U-slots and layered with an H-shaped parasitic patch (Abdi & Aguili, 2024; Khidhir, 2023). Wideband is produced by stacking rectangular patches that have been loaded with U-slots that are electromagnetically linked (Rajkumar & Usha, 2017). Recent research on multiband applications is attempting to reduce size by designing a single antenna rather than numerous antennas. Hence, a dual square-cut design for S-band and C-band wireless communication applications was presented in (Kadam et al., 2025). Moreover, because of the slot in the patch, the antenna with the first fractal iteration offers dual-band behavior. The antenna construction offers the dual-band functioning, and the patch's slot also functions as a resonating structure. As more slots are added to the structure, the antenna with the second fractal iteration offers triple-band functioning (Nhlengethwa & Kumar, 2021).

Therefore, instead of using many antennas for the same purpose, a single antenna functioning in the necessary band of frequencies is required, which makes multiband antennas applications possible and very effective in devices. Thus, an efficient substitute for broadband, high gain, and programmable antenna systems are small multiband antennas (Wa'il et al., 2022; Ibrahim, 2019; Liu et al., 2009; Kim et al., 2008). Therefore, it is necessary to find ways that lead to an improvement in these and other characteristics, and this is done through several changes in the composition of the antenna (Goyal et al., 2016). The most widely used technique is that embedding slots in conducting parts of various shapes (Jhamb et al., 2011). So, by reconfigurable the patch or ground plane of MSA one can get increasing in both the bandwidth and gain to use the antenna in the wide range of wireless communications applications such as Bluetooth, Wi-Fi, WLAN, WiMax (Konade & Dongre, 2024). Additionally, using this method, the researchers created new MSA structures with wideband and triple characteristics, particularly in the X-, Ku-, and K bands (Mutashar et al., 2022; Al-Tumah et al., 2020; Mishra, 2019; Yadav et al., 2018). The Multiple shapes of antenna patch have been used to create several working states for MSAs such as: wideband, dual- band, multi-band and miniaturization. As significant, the conducting patch can be any form, however the most widely utilized shapes are rectangular and circular (Fatemi-Nasab et al., 2021). One of the important methods of reconfiguring the patch was by using the concept of Fractal (Malallah et al., 2020; Reddy and Sarma, 2014). MSA fields, which are divided into mass and border fractals, have been greatly impacted by the fractal notion (Pen & Aziz, 2012). Antennas for wideband or multiband applications have been designed using mass fractals (Ali et al., 2018; Anguera et al., 2005). Compact antennas are designed using the space filling property of border fractals (Patel & Behera, 2025; Vinoy et al., 2003).

Satellites use "frequency bands" to relay data. Currently, C-band and Ku-band are the main commercial frequency bands in use. C-band is typically utilized for fixed services like PSN, Internet telecommunication, and mobile feeder lines, and it runs in the 4-6 GHz range. Rain, snow, and other meteorological conditions have little effect on transmissions. A transponder can typically send and receive data at a rate of 45 Mb/sec. Since these are analogy signal processors, the actual bandwidth a user can anticipate will depend on the modulation strategy. The typical width of a C-band transponder is 36 MHz. The first spectrum made available to satellites for communications was the traditional C-Band (Maral et al., 2020).

A novel design for a fractal square patch of MSA has been put forth in this study in order to get the wideband properties needed for multipurpose wireless applications. This suggested antenna's broad characteristics make it suitable for wireless applications such as WLAN and X-band and in high-performance spacecraft, satellite and missile. Moreover, enhanced procedures were provided to ensure high efficiency for the planned antenna. The suggested antenna was designed and simulated using a tool named Ansoft® High Frequency Structure Simulator (HFSS).

2. METHODOLOGY

In order to understanding the suggested antenna's geometry and configuration by using the Ansoft HFSS, there are some important principles and theoretical tools that are suitable to be presented. While designing the form of an antenna patch, one must consider how to link the patch's size to the radiation properties of the radiating element. Moreover, how the suggested patch would alter in impedance matching, bandwidth, gain, radiation pattern, and surface current distributions, which are represented the performance of proposed antenna (Khanna & Sharma, 2016; Kenenbaev et al., 2025). The fundamental component of an antenna that affects performance is the radiating patch, which modifies surface current distribution, bandwidth, and impedance matching. Patch antennas come in a variety of forms, which helps them function better as conducting patches in antennas. However, we made an effort to identify easier and more efficient methods to get the intended effects. In this paper, a square MSA has been presented as reference antenna of the proposed antenna with patch dimensions of 40x40 mm^2. The dielectric substrate for this antenna is composed of FR4-Epoxy and has a thickness of 1.59 mm and a dielectric constant of 4.4 and the ground plane overall dimensions are 79x50 mm^2. This antenna is feeding by the line strip technique. However, by selected the optimum antenna dimensions with size and location of fed type the good impedance matching has been obtained. Research in the fields of wireless communication has increased due to the growing need to design antennas for a variety of applications. Numerous classic and sophisticated wireless systems have been developed for a wide range of uses. These designs offer more dependable contacts and improved performance. Therefore, the wireless systems must enhance a number of factors, including frequency band, radiation pattern, return loss, VSWR, and gain, in order to accomplish this purpose. Recently, microstrip antennas have attracted a lot of research attention because of their high efficiency, ease of manufacturing, and light weight (Kallumottakkal et al., 2025).

2.1. Study Design

The suggested patch geometry is created and manufactured utilizing square patch which included etched spiral slots in addition to cutting half circle from each corner of square patch. These slots and half circles are simple symmetry shapes. Using HFSS software, Figure 1 illustrates the suggested antenna design process.

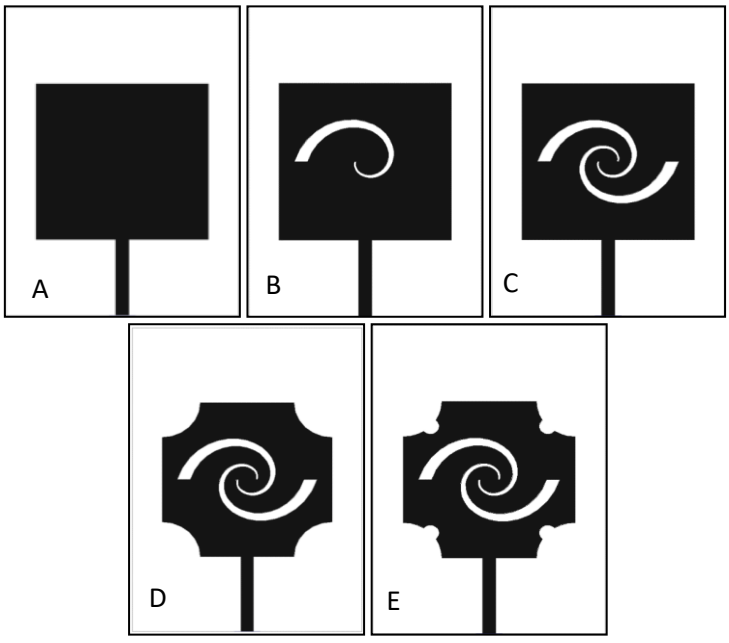

Figure 1. Steps to choosing the suggested antenna

First step represents MSA with square patch (Design A). Design B shows one spiral slot on the square patch. Similarly, second spiral slot is etched on the square patch with opposite direction to the first spiral slot, as a Design C. In the next step, half circle was cutting from each corner of square patch (Design D). Finally, small a half circles are cutting from inside the corners that were cut in the previous step (Design E). The standing wave ratio (1< VSWR < 2) and the return loss at -10 dB for each design were the factors that caused the patch to change from design A to design E. The best output values for both factors should be found in the ideal model. This indicates that when the transmission line and antenna line feed are close to or equal to 50 ohms, the matching is satisfactory. Conversely, the ideal radiation pattern with good beam width and gain is provided by the optimal current distribution. Design E performed the best when compared to the outcomes shown in the figures and tables. The surface of equiangular spiral is one geometrical configuration and described by angles. Furthermore, fulfils all shapes requirements are frequency independent. Therefore, we find that changing the equation of the curve with respect to the electrical dimension and the physical dimension gives the same results. Congruence can be established only by rotation in ϕ, and because of the symmetrical in both terminal along θ=0, π-axis, the rotation in θ is forbidden (Balanis, 2016).

The spiral slots are etched on the square patch as new-shaped of exponential slot, which have a curve equation form in HFSS according to the following mathematical relations:

$$X(U,\emptyset) = ((1-\emptyset)\times cc \times exp\,(alpha \times U \times \pi/180) + cc \times \emptyset \times exp(alpha \times (U-delta)\times \pi/180)) \times cos\left(U \times \frac{\pi}{180}\right) \quad (1)$$

$$Y(U,\emptyset) = ((1-\emptyset)\times cc \times exp(alpha \times U \times \pi/180) + cc \times \emptyset \times exp(alpha \times (U-delta)\times \pi/180)) \times sin(U \times \pi/180) \quad (2)$$

$$Z(U,V) = h \quad (3)$$

From these equations, the system composed of two equally ended arms (cc) and so that it forms a balanced system. The finite size of the structures is specified by the fixed spiralling length (l_1) along the centerline of the arm. The entire structure can be completely specified by the rotation angle (delta), the arm length (l_1) and the rate of expansion of the spiral (U). Also, the outer structure, but here depend on the angle between the radial distance (y2) and the tangent to the spiral (alpha) along the arm length. However, all equations parameter values are included in Table 1.

Table 1. The Proposed antenna's dimensions.

Patch		Spiral Slots		Feed	
Parameters	**Dimension**	**Parameters**	**Dimension**	**Parameters**	**Dimension**
Ws	50.00 mm	cc	2.5 mm	Wf	3.00 mm
Ls	79.00 mm	alpha	0.300 deg.	Lf	20.00 mm
Wp	40.00 mm	delta	40.00 deg.	(xf, yf)	(0.0mm,34.5mm)
Lp	40.00 mm	U	(0.0,1.0)	l1	40 mm
h	1.59 mm	∅	(0-360) deg.		
R1	9.00 mm	y1	5.0 mm		
R2	2.50 mm	y2	6.5 mm		

As demonstrated in the following section, Due to the positive simulation results of radiation pattern and return loss, the recommended antenna of Figure 1 (Design E) is selected as the optimum design. As clear in Figure 2, the antenna's dimensions are optimized by a parameterization study based on optimal performance using the HFSS software. This software is based on the finite element method and used for solving the problems of mathematical physics and engineering.

Figure 2 illustrates the geometrical design of the proposed antenna in order to achieve dual band, the best return loss value, and a good efficiency value. However, the dimensions and characteristics used in the design and fabrication of the proposed antenna are displayed in Table 1. Figure 3 illustrates the design and construction of the proposed antenna, which has been manufactured. This figure shows the experimental work involved fabricating antenna prototype using a CNC laser and then determining the antenna performance using a vector network analyzer ROHDE & SCHWARZ ZVA24, where measurement setup of parameters is completed inside the anechoic chamber.

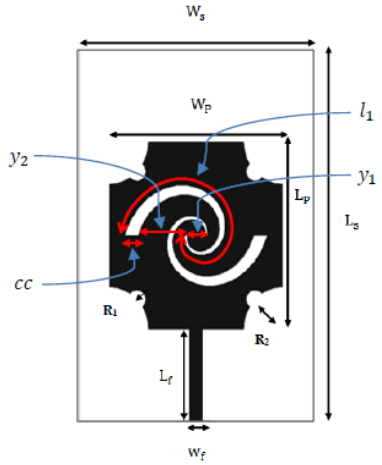

Figure 2. Geometrical of the proposed antenna (Design E)

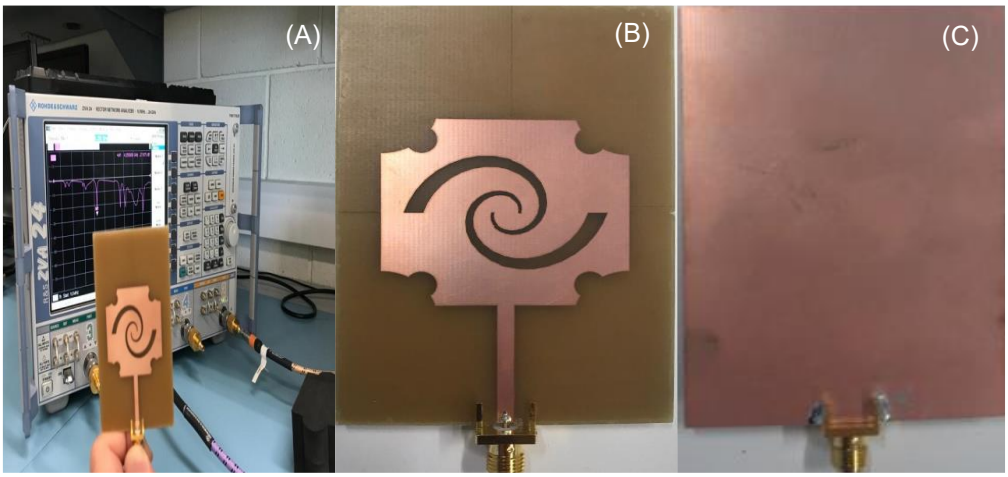

Figure 3. The proposed antenna setup(**A**) Measurement setup of parameters inside the anechoic chamber, (**B**) Top and (**C**) Bottom views of the manufactured antenna

3. RESULTS AND DISCUSSION

The procedures used to get the ideal final antenna design shape are depicted in Figure 1. in order to obtain positive qualitative outcomes. MSA is represented by a square patch in the first phase (Design A). The square patch in Design B has a single spiral slot. Similarly, as a Design C, the second spiral slot is etched on the square patch in the opposite direction from the first spiral slot. The next phase involved cutting a half circle from each square patch corner (Design D). Lastly, little half circles are being cut from inside the corners that were previously cut (Design E). The performance of the recommended antenna with various parametric features is examined in this study. The suggested antenna was designed and simulated using the HFSS software. With ideal dimensions as specified in Table 1, the suggested fractal square microstrip antenna based on spiral slots is displayed in Figure 2.

Table 2. Return loss features and average gain values of the proposed antennas

Proposed antenna	Bandwidth (GHz)	Resonance frequency (GHz)	Average Gain (dB)
Design A	0.09	1.76	1.70
	0.22	5.10	0.65
	0.40	7.00	4.43
Design B	0.36	3.40	1.00
	0.51	5.70	5.46
	0.89	9.00	1.20
Design C	0.80	6.96	4.77
	0.45	8.19	2.70
	1.08	9.14	2.95
Design D	0.48	7.10	7.40
	0.49	8.50	4.80
Design E	0.13	4.01	1.50
	2.85	7.10	5.73

In this study, a single antenna design is shown for downsizing and broadband applications rather than several antennas. Figure 2 illustrates the suggested antenna geometry, which was created and constructed to resonate in the C-band frequency. This antenna offers dual band characteristics as a result. In order to propose and build a small MSA design, the square MSA that contains spiral slots and fractal curves which are embedded on the proposed antenna patch. Surface currents have the appropriate phase reversal when spiral slots and fractal curves are the right sizes. Thus, the desired radiation patterns at the desired frequencies are being achieved by appropriately selecting phase reversal in surface currents. The results of the modeling of the return loss indicate that the suggested antenna performs better. Better impedance matching can be achieved by altering the surface current route through the use of fractal curves and spiral slots. As clear in Figure 2, the commercial application Ansoft HFSS has been used to model the proposed antenna. Double-sided plain copper resist board (RA-Ae16) with an economical FR4-Epoxy measuring (50×79) mm^2 is used to create the antenna, dielectric constant of εr = 4.4 and thickness of mm) and dimensions (3 mm,20 mm), as depicted in Figure 3. Table 2 shows the dimensions of the suggested antenna. This antenna is feeding by the strip line with dimensions 3.0 mm x 20.0 mm and a satisfactory matching of impedance has been achieved. at the feed point location at xf = 0.0 mm and yf = 34.5 mm. Figures 4 and 5 display the characteristics of the simulated return loss and VSWR of the suggested antennas in Figure 1, respectively. Additionally, Table 2 shows the values of the simulated return loss. Furthermore, the amount of power communicated in the high radiation trend are simulated by using of antenna gain definition. Because of the good simulation results of return loss and VSWR, Design E is chosen as the optimal design from Figures 4 and 5. The suggested antenna's construction validates these findings.

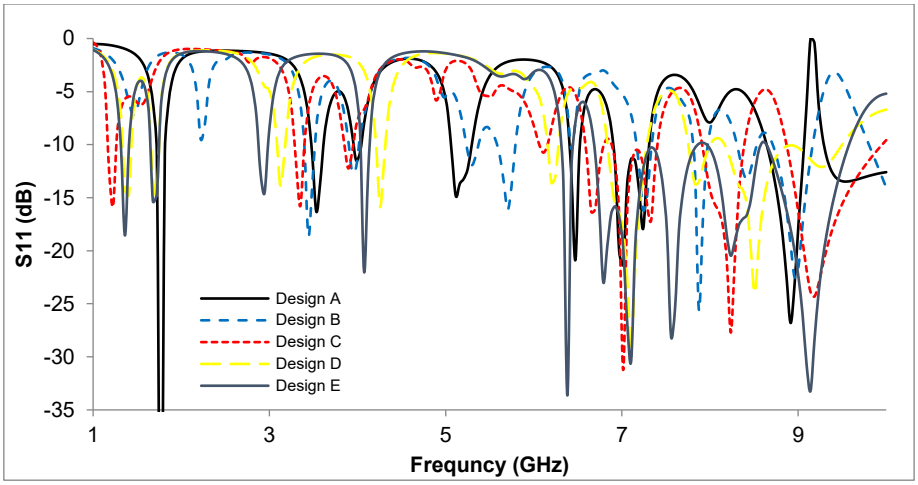

Figure 4. Return loss simulation results for the suggested antennas in Frame 1

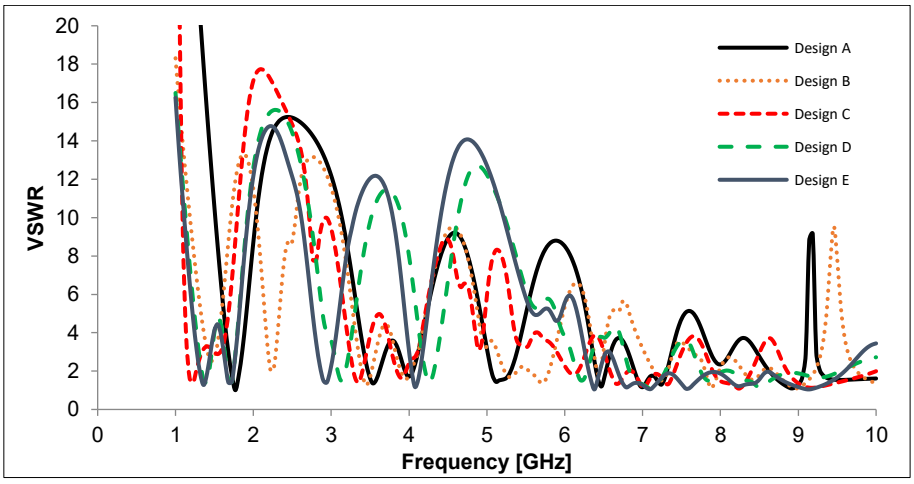

Figure 5. VSWR simulation result of the optimum designed antenna in Fig. 1

The vector network analyzer ROHDE & SCHWARZ ZVA24 was used to measured reflection coefficient S11 of fabricated antenna. The measured and simulated values of S11 are displayed in Figure 6. Dual band resonance is seen in the prototype antenna at 4.01 and 7.1 GHz with return loss -

18 dB and -33 dB, respectively. As observed in Figure 6, the simulation and measurement estimate of return loss were compared. In this figure 6, a little difference between the simulated and measured results may be caused due to the soldering effects used for the SMA connector, which is normally neglected in the simulation design. However, a good degree of agreement between the return loss estimates from the simulation and measurement is shown in Table 3.

At the resonance frequencies of 4.23 and 7.13 GHz, respectively, the simulated data shows a dual band with impedance bandwidths of 350 MHz (3.94−4.20 GHz) and 2750 MHz (6.96-9.55 GHz). The current investigation shown that, in comparison to the first frequency band, the second frequency band has a larger impedance bandwidth value. As a result, the suggested antenna is very helpful for C-band applications and has two impedance bandwidths that are situated within C-band.

Table 3. Comparison of the antenna design's simulated and measured return loss characteristics fonts and sizes

Proposed antenna	Resonant frequency (GHz)	Return loss (dB)	Bandwidth (MHz)
Simulated	4.01	-18.0	220
	7.10	-33.0	2850
Measured	4.23	-13.0	350
	7.13	-30.0	2750

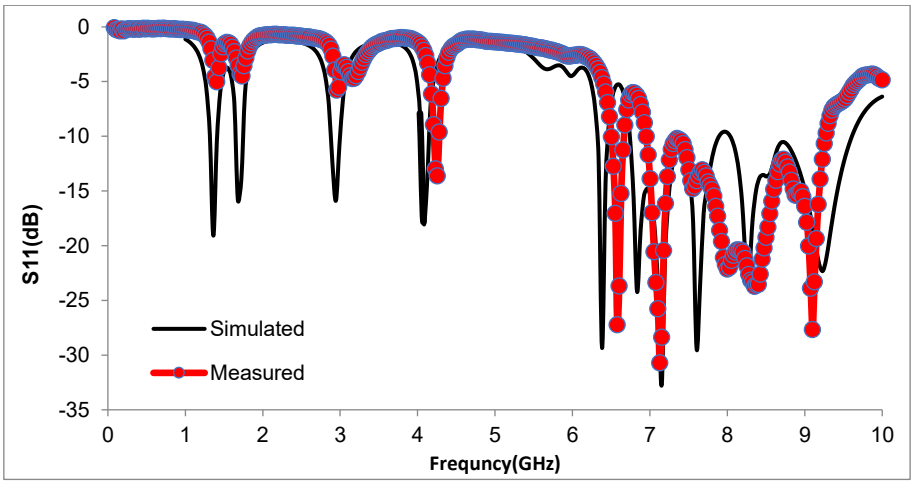

Figure 6. Simulated and measured return loss features of proposed antenna

In order to controlling the power transfer from fed source to the antenna, the impedance matching between connection points must be satisfy, because the input impedance is the most important parameter when design an antenna. Figure 7 shows the input impedance simulation results for the suggested antenna as a function of frequency. The simulated input impedance values are near 50 Ω, as this figure illustrates. Furthermore, at the resonant frequencies, the observed and simulated impedance values 4.01 GHz and 7.1 GHz are depicted in Table 4, which illustrated the comparison between the simulated and measured finding of input impedance.

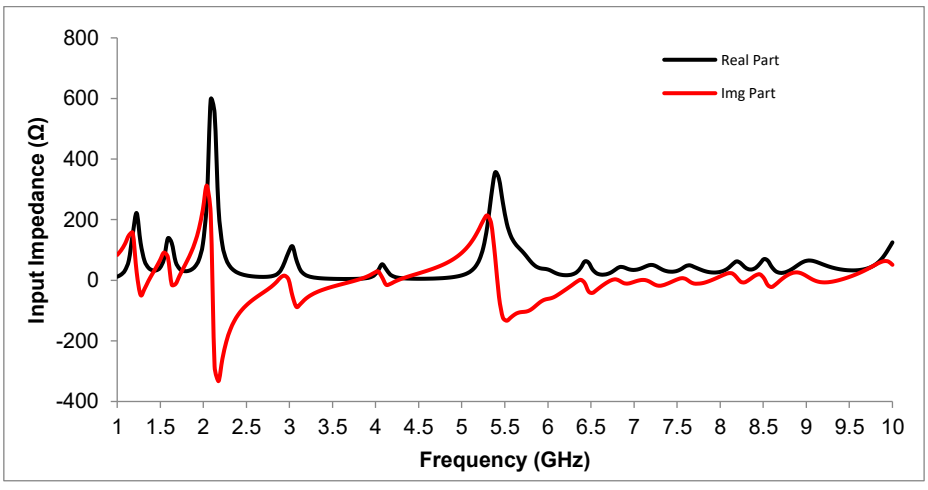

Figure 7. Input impedance simulation results for the best-designed antenna

Table 4. Comparison of the simulated and measured values of input impedance of the antenna designed

Proposed antenna	Resonant frequency (GHz)	Input impedance (Ω)
Simulated	4.01	(52.0 , -3.0)
	7.10	(48.0 , 1.0)
Measured	4.23	(52.0 , -3.0)
	7.13	(48.0 , 1.0)

The electric surface current density and fields (E&H) distribution on the patch of the optimum designed antenna at 4.01 and 7.1 GHz are shown in Figures 8 and 9, respectively. The strongest current distribution is depicted in this figure is along the spiral slot and the high of fractal curves. However, the behaviour of the related surface currents is validated by the electric and magnetic fields. For this reason, the fields increasing will be caused from the surface currents and take the maximum value in some points and minimum on other depending on currents phase. The distribution of electric and magnetic fields on the optimally built antenna is depicted in Figures 8(B), (C) and 9(B), (C).

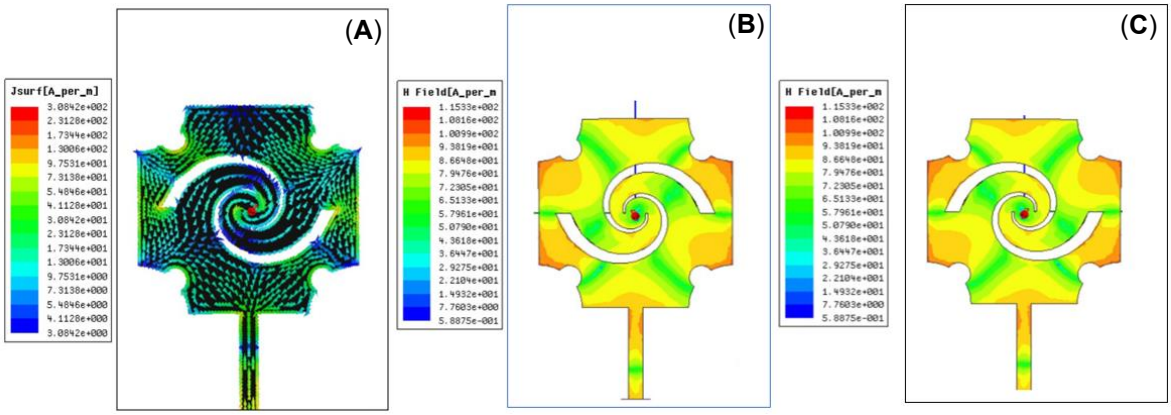

Figure 8. (**A**) Surface currents distribution, (**B**) electric and (**C**) magnetic fields on the antenna patch of design (E) at 4.01 GHz

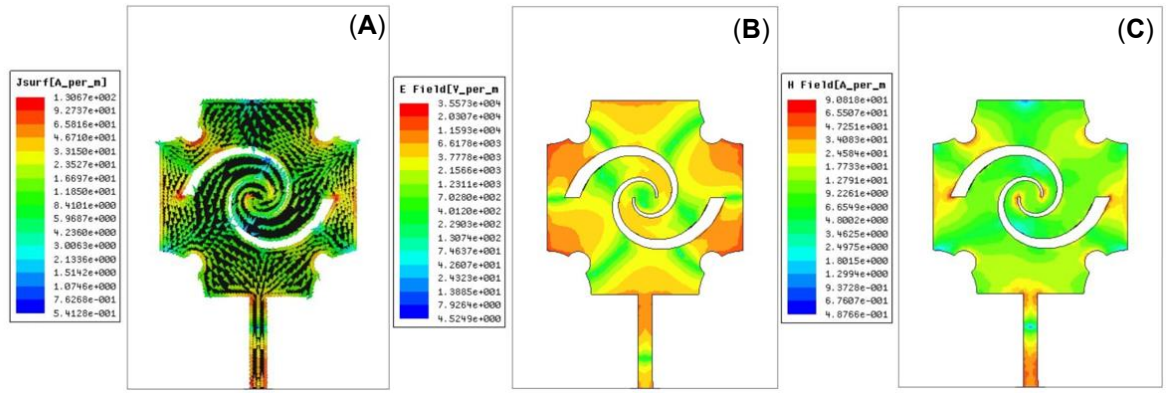

Figure 9. (**A**) Surface currents distribution, (**B**) electric and (**C**) magnetic fields on the antenna patch of design (E) at 7.10 GHz

Figure 10 shows the simulated results of radiation pattern in 2D- and 3D- for the optimum antenna design (E) at both resonant frequencies 4.01 and 7.10 GHz. The E-plane and H-plane half power beamwidths at the resonant frequencies in this figure are (62^{o} and 92^{o}) and (45^{o} and 51^{o}), respectively. For wireless applications, the suggested antenna's radiation pattern characterizations are necessary. Figure 11 shows the efficiency of the proposed antenna as a function of operating frequencies as predicted by HFSS. Moreover, this figure illustrates the radiation efficiency of the proposed antenna 60%.

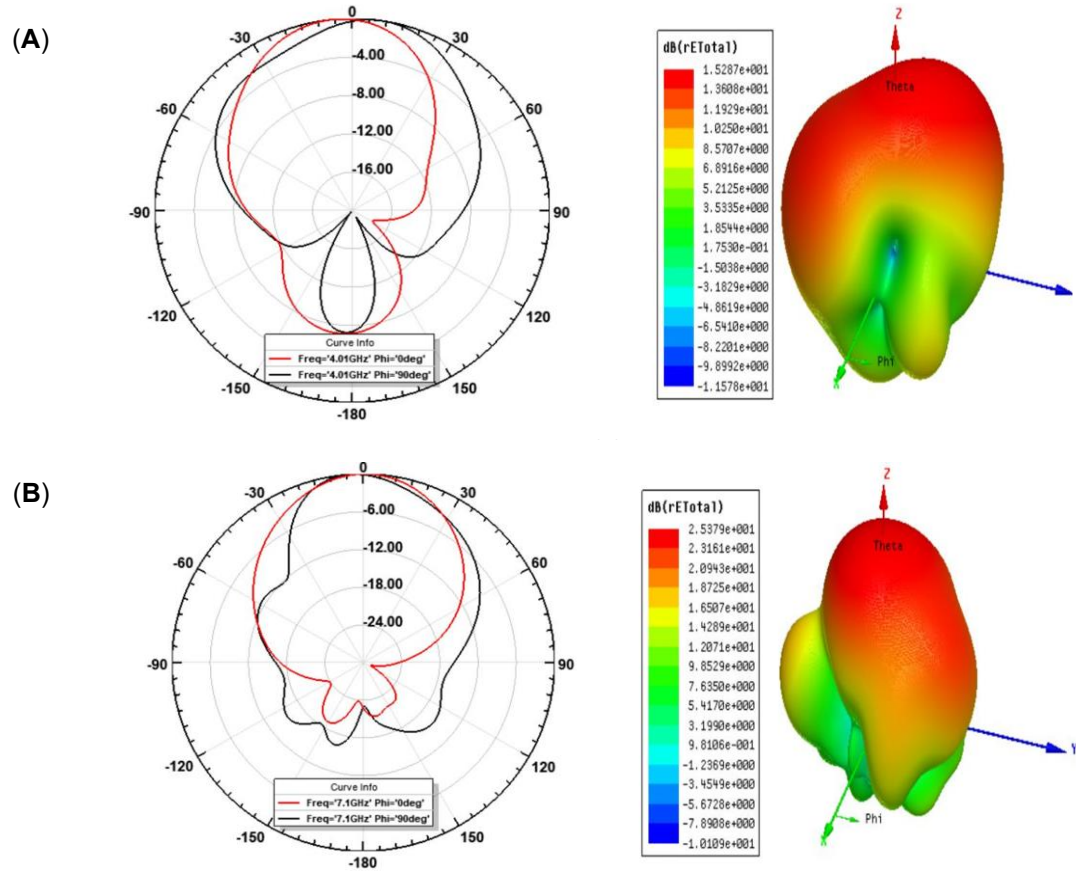

Figure 10. Simulated results of radiation patterns of the proposed antenna design (E) at (**A**) 4.01 GHz and (**B**) 7.1 GHz

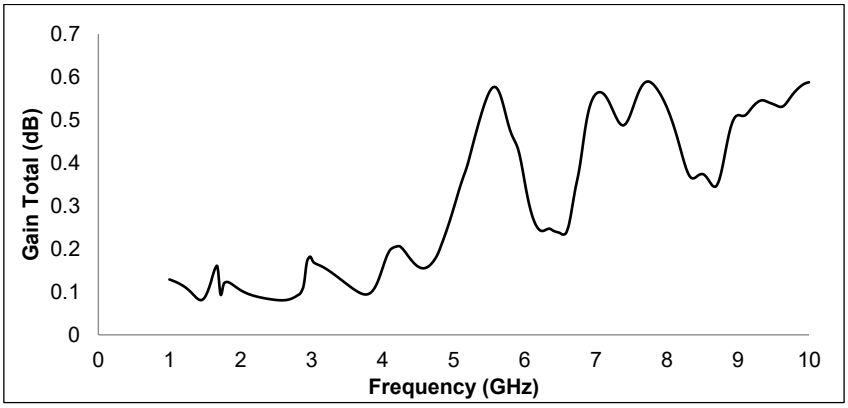

Figure 11. The antenna radiation efficiency as a function of operating frequencies using HFSS

Table 5 presents a comprehensive comparison between the performance of some recently developed antennas for S-, C- and X-bands applications and the proposed antenna in this paper. The comparison includes material and a range of performance metrics such as S11, antenna dimensions, impedance bandwidth, and gain. our proposed antenna demonstrates better performance in terms of both gain and impedance bandwidth.

Table 5. Comparison of the antenna design's simulated and measured return loss characteristics fonts and sizes

References	Antenna Size (mm3)	Material (substrate)	Frequency (GHz)	S11 (dB)	Gain (dBi)	BW (GHz)
This work	50×79×1.59	FR4	4.01 , 7.10	-18, -33	1.5, 5.73	0.13 , 2.85
Lakrit, 2018	42×42×3.2	Rogers RT/duroid	2.54	-22	-	0.162
Nhlengethwa & Kumar 2021	16×18×1.6	FR4	7.24,11.08	-23.6,-17.16	5.36,4.65	0.25 , 0.74
Reddy & Sarma, 2014	57.9×57.9×1.5	FR4	4.9 , 5.3	-18, -22	2.67,1.48	0.35 , 0.61
Kadam et al., 2025	48×68×1.53	FR4	2.482 , 5.8	-38, -26.5	-	1.53 , 2.17

4. CONCLUSION

Fractal patch of MSA is designed and fabricated using square patch which included etched spiral slots in addition to cutting half circle from each corner of square patch for wideband applications, with size of 79×50×1.59 mm^3. To achieve appropriate impedance matching, these slots are positioned and sized optimally. With dual band characteristics, the novel patch antenna can generate new resonance frequencies. The return loss features are measured and display dual band with impedance bandwidth of 350 and 2750 MHz at the resonance frequencies 4.23 and 7.13 GHz, respectively. Compared to the first frequency band, the second impedance bandwidth is obviously larger. For C-band applications, the suggested antenna is therefore preferred. The highlight of implication is the novel design has two impedance bandwidths located within C-band, radiation patterns characteristics of the proposed antenna are desired for wireless applications, the new patch antenna provides accepted values of the antenna gain and a large value of the impedance bandwidth was obtained at C-band. Two separate frequency bands of operation are shown by the simulation results: the first band, which spans 3.94 to 4.20 GHz (S-band), has a bandwidth of about 260 MHz, and the second band, which spans 6.96 to 9.55 GHz (C- and X-bands), has a bandwidth of around 2.85 GHz. The antenna is appropriate for S-band, C-band, and X-band wireless communication applications due to its dual-band performance. According to simulation results, the antenna can operate effectively over S-, C-, and X-band frequencies with a VSWR of less than two and a return loss of less than -10 dB. For an antenna to be useful in the wireless field, these specifications are adequate.

ACKNOWLEDGEMENT
This work was supported by Dr. Ra'ed A. Malallah in UCD Centre for Precision Surgery, University College Dublin, Ireland for his scientific cooperation. Also, the authors thank University of Basrah, College of Science, for their continuous support and encouragement during this work. Thanks for the help provided to successfully complete this research.

CONFLICT OF INTEREST
The authors declare no conflicts of interest.

AUTHOR CONTRIBUTION
Akeel Tahir and Wa'il Al-Tumah conceived of the presented idea, developed the simulation and performed the computations. Akeel Tahir, Doha Al-Feadh and Alistair P. Duffy discussed the results. Akeel Tahir, Wa'il Al-Tumah and Alistair P. Duffy wrote the manuscript and approved the final article.

DATA AVAILABILITY
All data generated or analyzed during this study are included in this published article.

DECLARATION OF GENERATIVE AI
Not applicable.

ETHICS
Not applicable.

REFERENCES

Abdi M, Aguili T. (2024). Unveiling the diverse applications and problem-solving capabilities of the MOM-GEC hybrid approach: a comprehensive systematic review. *Journal of Computational Electronics*, 23, 791-818. doi:10.1007/s10825-024-02169-2

Ali T, Aw MS, Biradar RC. (2018). A fractal quad-band antenna loaded with -shaped slot and metamaterial for applications. *International Journal of Microwave and Wireless Technologies*, 10, 826-834. doi:10.1017/S1759078718000272

Al-Tumah WAG, Shaaban RM, Ahmed ZA. (2020). Designing a microstrip patch antenna in part of ultra-wideband applications. *Baghdad Science Journal*, 17(4), 19. doi:10.21123/bsj.2020.17.4.1216

Anguera J, Puente C, Borja C, Soler J. (2005). Fractal shaped antennas: A review. *Encyclopedia of RF and Microwave Engineering,* 2, 1620-1635. doi:10.1002/0471654507.eme128

Balanis CA. (2016). Antenna theory: analysis and design. John wiley & Sons, p. 543-549.

David M. (1995). Techniques for Microstrip Antennas. Microstrip Antennas: the analysis and design of microstrip antennas arrays. The Institute of Electrical and Electronics Engineers, New York.

Deschamps GA. (1953). Microstrip microwave antennas. In Proceedings of the Third Symposium on the USAF Antenna and Development Program, p 18-22.

Elalaouy O, El Ghzaoui M, Foshi J. (2024). Enhancing antenna performance: A comprehensive review of metamaterial utilization. *Materials Science and Engineering: B*, 304, 117382. doi.10.1016/j.mseb.2024.117382

Fatemi-Nasab J, Jarchi S, Keshtkar A. (2021). Complementary split ring resonator effects on radiation pattern reconfigurable circular microstrip antennas. *Iranian Journal of Electrical and Electronic Engineering*, 17(1), 1-11. doi.10.22068/IJEEE.17.1.1775

Gao P, Xiong L, Dai J, He S, Zheng Y. (2013). Compact printed wide-slot UWB antenna with 3.5/5.5-GHz dual band -notched characteristics. *IEEE Antennas and Wireless Propagation Letters*, 12, 983-986. doi.org/10.1109/LAWP.2013.2277591

Goyal A, Gupta A, Agarwal L. (2016). A review paper on circularly polarized microstrip patch antenna. *International Journal of New Technology and Research*, 2(3), 138-142.

Howell J. (2003). Microstrip antennas. *IEEE Transactions on Antennas and Propagation*, 23, 90-93. doi:10.1109/TAP.1975.1141009

Ibrahim IM. (2019). Compact MIMO slots antenna design with different bands and high isolation for 5G smartphone applications. *Baghdad Science Journal*, 16(4), 1093-1102. doi:10.21123/bsj.2019.16.4(Suppl.).1093
James JR, Hall PS. (1989). Handbook of microstrip antennas. Peter Peregrinus Ltd., United Kingdom, p. 45-110.
Kadam S, Desai KR, Pawar AP, Pawar S, Nigade A. (2025). Design and performance of two stages square cut rectangular multiband microstrip fractal antenna. *MethodsX*, p.103559, 1-11. doi:10.1016/j.mex.2025.103559
Kallumottakkal M, Farade RA, Jawaid M, Al Ahmad M, Wahab NIA, Khan TY, Shaik AS. (2025). radio frequency energy harvesting: a review on progress and development, applications, and sustainability benefits. *Materials Today Sustainability*, 101291, 1-53. doi:10.1016/j.mtsust.2025.101291
Karanam R, Kakkar D. (2025). Design and implementation of a fractal microstrip patch array for vehicle-to-vehicle communication using meta-heuristic techniques. *Journal of Computational Electronics*, 24(4), 110. doi:10.1007/s10825-025-02355-w
Kenenbaev E, Kenenbaeva G, Abakirova G, Nazarbaev F. (2025). functional relations as a tool for analysing differential equations. *Journal of Science and Mathematics Letters*, 13(2), 72-86. doi:10.37134/jsml.vol13.2.6.2025
Khanna G, Sharma N. (2016). Fractal antenna geometries: A review. *International Journal of Computer Applications*, 153(7), 29-32. doi:10.5120/ijca2016912106
Khidhir AH. (2023). Implementation of a circular shape patch antenna at 2.4 GHz for different wireless communications. *Iraqi Journal of Science*, 64(1), 205-214. doi:10.24996/ijs.2023.64.1.21
Kim SC, Lee SH, Kim YS. (2008). Multi-band monopole antenna using meander structure for handheld terminals. *Electronics Letters*, 44(5), 331-332. doi:10.1049/el:20080004
Konade S, Dongre M. (2024). Compact Two-Port MIMO Antenna with High Isolation for UWB Applications. *Iranian Journal of Electrical & Electronic Engineering*, 20(2), 1-9.
Lakrit S. (2018). Design of dual and wideband rectangular patch antenna for C and X band applications. *Advanced Electromagnetics*, 7(5), 145-150. doi:10.7716/aem.v7i5.933
Liu WC, Ghavami M, Chung WC. (2009). Triple-frequency meandered monopole antenna with shorted parasitic strips for wireless application. *IET Microwaves, Antennas and Propagation*, 3(7), 1110-1117. doi:10.1049/iet-map.2008.0204
Malallah RE, Shaaban RM, Wa'il AG. (2020). A dual band star-shaped fractal slot antenna: Design and measurement. *AEU-International Journal of Electronics and Communications*, 127, 153473, 1-9. doi:10.1016/j.aeue.2020.153473
Maral G, Bousquet M, Sun Z. (2020). Satellite communications systems: systems, techniques and technology. John Wiley & Sons, p. 56-65.
Mishra B. (2019). An ultra compact triple band antenna for X/Ku/K band applications. *Microwave and Optical Technology Letters*, 61(7), 1857-1862. doi:10.1002/mop.31812
Mutashar RA, Tahir AS, Wa'il AG. (2022). Enhancement the gain and bandwidth of a circular patch microstrip antenna in X-band. In AIP Conference Proceedings, AIP Publishing LLC. doi:10.1063/5.0121529
Muthuvalu MS, Sulaiman J. (2010). Quarter-Sweep Iterative Method for Second Kind Linear Fredholm Integral Equations. *Journal of Science and Mathematics Letters*, 2(1), 67-77.
Nguyen DT, Lee DH, Park HC. (2012). Very compact printed triple band-notched UWB antenna with quarter-wavelength slots. *IEEE Antennas and wireless propagation letters*, 11(3), 411-414. doi:10.1109/LAWP.2012.2192900
Nhlengethwa NL, Kumar P. (2021). Fractal microstrip patch antennas for dual-band and triple-band wireless applications. *International Journal on Smart Sensing and Intelligent Systems*, 14(1), 1-9. doi:10.21307/ijssis-2021-007
Patel K, Behera SK (2025). Design of band reconfigurable Koch fractal antenna for wideband applications. *AEU-International Journal of Electronics and Communications*, 188, 155592. doi:10.1016/j.aeue.2024.155592
Pen CC, Aziz ZA, (2012). Results relating to Hirota Method and singularity analysis on some nonlinear waves equations. *Journal of Science and Mathematics Letters*, 4(1), 75-83.
Rajkumar R, Usha KK. (2017). A metamaterial inspired compact open split ring resonator antenna for multiband operation. *Wireless personal communications*, 97(1), 951-965. doi:10.1007/s11277-017-4545-0
Reddy VV, Sarma NVSN. (2014). Compact circularly polarized asymmetrical fractal boundary microstrip antenna for wireless applications. *IEEE Antennas and Wireless Propagation Letters*, 13, 118-121. doi:10.1109/LAWP.2013.2296951
Sharma P, Vaish A, Yaduvanshi RS. (2019). The design of a turtle-shaped dielectric resonator antenna for ultrawide-band applications. *Journal of Computational Electronics*, 18(4), 1333-1341. doi:10.1007/s10825-019-01374-8
Siakavara K. (2011). Methods to design microstrip antennas for modern applications. Microstrip Antennas. Intech Open, Croatia, p. 173-236.
Srivastava DK, Saini JP, Chauhan DS. (2009). Broadband stacked H-shaped patch antenna. *International Journal of Recent Trends in Engineering*, 2(5), 385-389.
Vinoy KJ, Abraham JK, Varadan VK. (2003). On the relationship between fractal dimension and the performance of multi-resonant dipole antennas using Koch curves. *IEEE Transactions on Antennas and Propagation*, 51(9), 2296-2303. doi:10.1109/TAP.2003.816352
Wa'il AG, Shaaban RM, Duffy AP. (2022). Design, simulation, and fabrication of a double annular ring microstrip antenna based on gaps with multiband feature. *Engineering Science and Technology, an International Journal*, 29, 101033. doi:10.1016/j.jestch.2021.06.013
Wa'il AG, Shaaban RM, Tahir AS. (2020). Design, simulation and measurement of triple band annular ring microstrip antenna based on shape of crescent moon. *AEU-International Journal of Electronics and Communications*, 117, 153133. doi:10.1016/j.aeue.2020.153133
Yadav S, Jaiswal K, Patel AK, Singh S, Pandey AK, Singh R. (2018). Notch-loaded patch antenna with multiple shorting for X and Ku band applications. In Recent Trends in Communication, Computing, and Electronics: Select Proceedings of IC3E 2018. Springer Singapore. doi:10.1007/978-981-13-2685-1_12